JVSTA Journal of Vacuum Science & Technology A

Sintered Cr/Pt and Ni/Au ohmic contacts to B12P2

Clint D. Frye, Sergei O. Kucheyev, James H. Edgar, Lars F. Voss, Adam M. Conway, Qinghui Shao, and Rebecca J. Nikolić

Citation: Journal of Vacuum Science & Technology A **33**, 031101 (2015); doi: 10.1116/1.4917010
View online: http://dx.doi.org/10.1116/1.4917010
View Table of Contents: http://scitation.aip.org/content/avs/journal/jvsta/33/3?ver=pdfcov
Published by the AVS: Science & Technology of Materials, Interfaces, and Processing

Sintered Cr/Pt and Ni/Au ohmic contacts to $B_{12}P_2$

Clint D. Frye[a)]
Lawrence Livermore National Laboratory, Livermore, California 94550 and Department of Chemical Engineering, Kansas State University, Manhattan, Kansas 66506

Sergei O. Kucheyev
Lawrence Livermore National Laboratory, Livermore, California 94550

James H. Edgar
Department of Chemical Engineering, Kansas State University, Manhattan, Kansas 66506

Lars F. Voss, Adam M. Conway, Qinghui Shao, and Rebecca J. Nikolić[b)]
Lawrence Livermore National Laboratory, Livermore, California 94550

(Received 29 January 2015; accepted 24 March 2015; published 9 April 2015)

Icosahedral boron phosphide ($B_{12}P_2$) is a wide-bandgap semiconductor possessing interesting properties such as high hardness, chemical inertness, and the reported ability to self-heal from irradiation by high energy electrons. Here, the authors developed Cr/Pt and Ni/Au ohmic contacts to epitaxially grown $B_{12}P_2$ for materials characterization and electronic device development. Cr/Pt contacts became ohmic after annealing at 700 °C for 30 s with a specific contact resistance of 2×10^{-4} Ω cm^2, as measured by the linear transfer length method. Ni/Au contacts were ohmic prior to any annealing, and their minimum specific contact resistance was ~l–4 × 10^{-4} Ω cm^2 after annealing over the temperature range of 500–800 °C. Rutherford backscattering spectrometry revealed a strong reaction and intermixing between Cr/Pt and $B_{12}P_2$ at 700 °C and a reaction layer between Ni and $B_{12}P_2$ thinner than ~25 nm at 500 °C. © *2015 American Vacuum Society*.
[http://dx.doi.org/10.1116/1.4917010]

I. INTRODUCTION

Boron and phosphorus form two distinct semiconductor compounds, cubic zincblende boron phosphide (BP) and rhombohedral $B_{12}P_2$, which in addition to having different stoichiometries also have different crystal structures and electronic properties. $B_{12}P_2$, often called icosahedral boron phosphide, is a wide-bandgap semiconductor [$E_g = 3.35$ eV (Ref. 1)] composed of boron icosahedra with interlinking phosphorus–phosphorus chains. It possesses many properties such as high hardness and chemical inertness that make it desirable as a semiconductor that can withstand extreme environments. Moreover, $B_{12}P_2$ can reportedly self-heal from intense beta-irradiation.[2,3] This unusual property makes $B_{12}P_2$ very attractive for a number of technologies, including radiation detection, electronics in harsh radiation environments, and radioisotope batteries—devices that directly convert nuclear energy into electricity.

Recent advancements in the improved heteroepitaxial growth of a similar rhombohedral boride, $B_{12}As_2$, have been achieved on SiC, including suppression of double-position twinning[4,5] and control of *p*-type doping[6] (note: *n*-type conductivity in neither $B_{12}P_2$ nor $B_{12}As_2$ has been reported yet). Heterojunction *pn*-diodes of *p*-$B_{12}As_2$/*n*-SiC have also been demonstrated.[7] However, before $B_{12}P_2$ diodes can be fabricated and characterized, a process for creating low resistance ohmic contacts to *p*-type $B_{12}P_2$ must be developed.

For many wide-bandgap materials, forming a low resistance ohmic contact is challenging. For instance, *p*-type GaN contacts typically have specific contact resistances on the order of 10^{-4}–10^{-6} Ω cm^2.[8] Ino *et al.*[9] recently published a study on the electrical characteristics of various metal contacts to *n*-type ($n \sim 10^{19}$ cm^{-3}) cubic BP, reporting specific contact resistances of 10^{-2}–10^{-5} Ω cm^2. Wang *et al.*[10] developed Cr/Pt ohmic contacts with a specific contact resistance of 3×10^{-4} Ω cm^2 to $B_{12}As_2$ by annealing at 700 °C. However, there is little data in the literature on metal contacts to $B_{12}P_2$. Use of sintered Al has been mentioned in multiple publications by Kumashiro *et al.*,[11,12] and while Si has been used to form a heterojunction diode with $B_{12}P_2$,[13] the current–voltage characteristics display a nearly ohmic relationship.

While studies on ohmic contacts to BP and $B_{12}As_2$ have been reported, this is the first study on the characterization of ohmic contacts to $B_{12}P_2$, which will enable further material characterization and development of functional $B_{12}P_2$ electronic devices. Here, Cr/Pt and Ni/Au ohmic metal-$B_{12}P_2$ contacts have been developed. Since Cr/Pt forms ohmic contacts to $B_{12}As_2$,[10] the same metal scheme was tested to determine if the process could be extended to $B_{12}P_2$. Additionally, Cr forms conductive borides[14] and phosphides[15] of varying composition that are stable to high temperatures.[16,17] Pt also alloys with both B and P, even forming eutectics below 600 °C.[18,19] Ni/Au, a well-established ohmic contact to *p*-type GaN,[8] was chosen as an alternate metal scheme. Like Cr, Ni forms various stoichiometries of electrically conductive Ni-B alloys[20] and nickel phosphides.[21] Further, Ni readily reacts with and/or dissolves both BP and $B_{12}P_2$,[22–25] aiding in the sintering process. However, the nickel phosphides and borides have melting points at temperatures above 800 °C, which may lead to

[a)]Electronic mail: frye6@llnl.gov
[b)]Electronic mail: nikolic1@llnl.gov

stability at higher temperatures than Cr/Pt. In addition, Ni has a large work function, which may reduce the barrier height. A top Au layer was used to provide a conductive oxide barrier for probing.

II. EXPERIMENTAL METHODS AND PROCESSING

$B_{12}P_2$ was grown epitaxially on on-axis (0001) 6H-SiC substrates via the thermal decomposition of B_2H_6 and PH_3 in H_2 at 1300 °C and a pressure of 100 Torr. Si-face, *c*-plane SiC was chosen due to its relatively low lattice mismatch of 2.54% and high thermal stability compared to Si. A detailed report on the epitaxial growth of $B_{12}P_2$ on SiC will be provided in a future publication. To prevent current flow through the substrate during electrical measurements, vanadium-doped, semi-insulating SiC was used. The $B_{12}P_2$ films were nominally 2 μm thick as measured by cross-sectional SEM. The hole concentration was $8 \times 10^{18}\,cm^{-3}$ as determined from Hall Effect measurements using the van der Pauw method and Ni/Au ohmic contacts fabricated as described below.

Annealing epitaxial $B_{12}As_2$ above 600 °C drastically reduces its sheet resistance.[6,10] This effect has also been observed in $B_{12}P_2$ films grown in our group, which may influence the electrical properties of the metal-semiconductor interface independently of any sintering effects. To decouple the effects of annealing-induced changes in the sheet resistance from the sintering of metal contacts, the $B_{12}P_2$ films were annealed in Ar at 800 °C for 30 s before any metal contacts were deposited.

Cr/Pt (500 Å/1000 Å) and Ni/Au (1000 Å/1000 Å) were evaluated as ohmic contacts to $B_{12}P_2$. The sheet resistance and specific contact resistance were measured by the linear transfer length method (TLM). The TLM patterns nominally consisted of $100 \times 100\,\mu m^2$ metal pads separated by spacings of 5, 10, 25, 40, 50, and 75 μm (see the inset of Fig. 1).

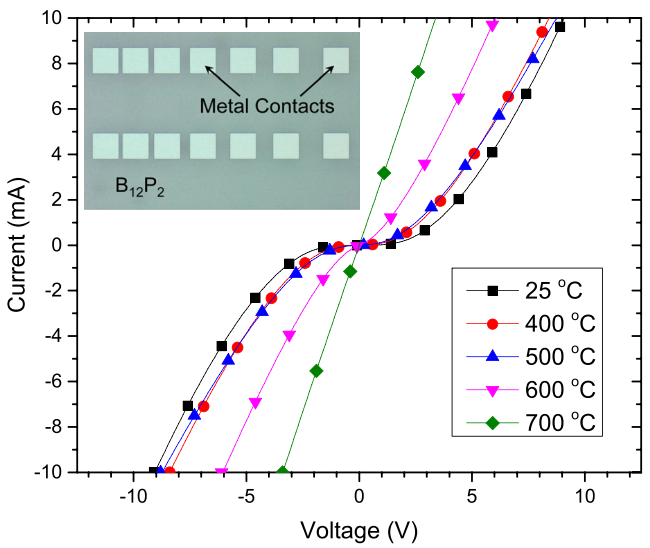

FIG. 1. (Color online) Progression of the current–voltage curve for Cr/Pt contacts with a spacing of 10 μm as they are annealed at subsequently higher temperatures, as indicated in the legend. Inset is an optical micrograph of two sets of TLM patterns. Each metal pad is nominally $100 \times 100\,\mu m^2$.

The metal contacts were formed via photolithography and electron-beam evaporation. The $B_{12}P_2$ films were cleaned in an O_2 plasma, dipped in buffered oxide etch for 10 s, quickly rinsed in deionized water, and blown dry with N_2 immediately prior to loading into the electron-beam evaporator.

After the metal was patterned, the samples were annealed in Ar in a rapid thermal annealing furnace. The films were annealed for 30 s at sequentially higher temperatures in 100 °C increments. Current–voltage (*I-V*) measurements were taken after each anneal on three adjacent sets of TLM patterns. The purpose of these measurements was to determine the minimum anneal temperature needed to form ohmic contacts for a given metal scheme and to test the effect of anneal temperature on the specific contact resistance. After ohmic conduction was achieved, the contact resistance was extracted from the current–voltage plots in the range of −1 V to +1 V with standard techniques.[26]

Because Rutherford backscattering spectrometry (RBS) is a nondestructive technique that provides depth-resolved information on individual elements independently of one another, it was employed to study the interface between the metals and $B_{12}P_2$ and to delineate the diffusion of metals into $B_{12}P_2$ and/or the diffusion of B or P into the metal. Since RBS may induce changes in the electrical properties of the film or contacts, separate samples were used for RBS analysis. Measurements were repeated on the same samples before and after annealing. They were done with a 2 MeV $^4He^+$ ion beam incident normal to the sample surface and a detector located at 164° from the incident beam direction.

III. RESULTS AND DISCUSSION

The conduction mechanism between a metal and a semiconductor can be predicted by comparing the thermal energy, kT, with the characteristic energy, E_{00}, which is a strong function of the carrier concentration.[27] For $B_{12}P_2$ with a hole concentration of $8 \times 10^{18}\,cm^{-3}$, $E_{00} \approx kT$. In this case, the conduction mechanism is in the thermionic field emission regime prior to sintering.

Despite the high background doping level in the $B_{12}P_2$ films, the carrier concentration is not large enough to facilitate pure field emission. Thus, the barrier height must be lowered by choosing a high work function metal or the contacts must react with and/or effectively dope the surface of the $B_{12}P_2$ film to induce ohmic conduction. With this information in mind, Cr/Pt and Ni/Au are evaluated. The results are summarized in Table I.

TABLE I. Work function, optimum anneal temperature (for 30 s anneals), and the corresponding specific contact resistance for the metals studied here.

	Cr/Pt 500 Å/1000 Å	Ni/Au 1000 Å /1000 Å
Work function (Ref. 28)	4.5/5.65 eV	5.15/5.1 eV
Anneal temperature	700 °C	500 °C
Specific contact resistance	$2 \times 10^{-4}\,\Omega\,cm^2$	$3 \times 10^{-4}\,\Omega\,cm^2$

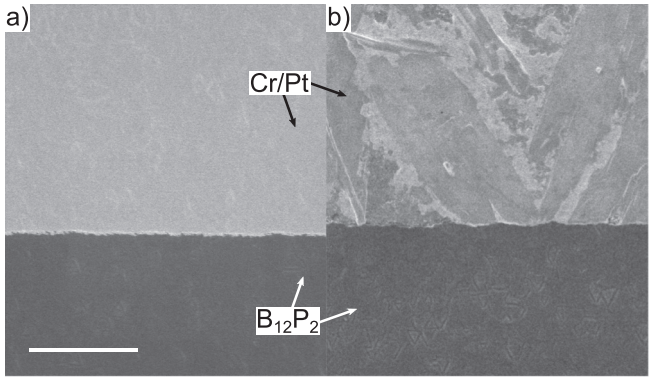

FIG. 2. SEM micrograph of Cr/Pt contact edges (a) before annealing and (b) after annealing at 700 °C for 30 s. The contact is smooth and uniform prior to annealing, and the morphology of the contact becomes much rougher after the anneal. The scale bar is 6 μm.

A. Cr/Pt contacts

Cr/Pt contacts were annealed at 400, 500, 600, and 700 °C for 30 s at each temperature. After annealing at 700 °C, conduction became ohmic. The progression of the *I-V* characteristics can be seen in Fig. 1. The *I-V* curve changes only slightly after the 400 and 500 °C anneals but becomes progressively linear after the 600 and 700 °C anneals. At 700 °C, the Cr/Pt contacts visibly react with the $B_{12}P_2$ film, apparently even wetting it [Fig. 2(b)]. Cr does not form a eutectic with B, P, or Pt below 1300 °C (Refs. 16, 17, and 29) and by itself is unlikely to cause wetting of the contact to the semiconductor. However, Pt readily forms phosphides that have melting points below 700 °C and as low as 590 °C.[19] The temperature of these phase changes corresponds well to the changes in electrical properties and surface morphology observed here.

Figure 3 shows the RBS spectra collected before any heat treatment of the contacts and after annealing at 700 °C for 30 s. Prior to annealing, Cr and Pt form discrete peaks,

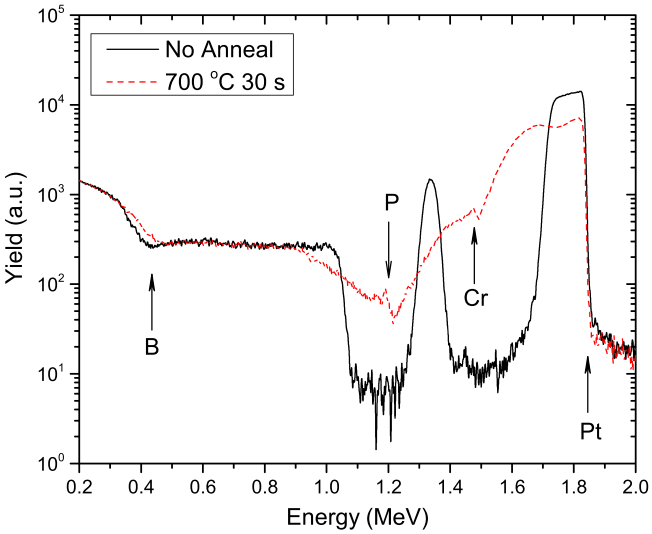

FIG. 3. (Color online) Semi-log plot of RBS spectra for Cr/Pt contacts before any heat treatment and after annealing at 700 °C for 30 s. The positions of the surface peaks of Pt, Cr, P, and B are denoted by arrows.

corresponding to nonintermixed Cr and Pt layers. Also, sharp B and P edges can be identified. The signals of the Cr, P, and B edges (roughly located at 1.36, 1.05, and 0.35 MeV, respectively) are shifted to energies lower than the surface peak energies denoted by arrows in Fig. 3 because they are not located at the sample surface but are buried beneath other layers. After annealing, Cr, Pt, P, and B peaks are dramatically broadened. The large Pt shift to lower energies (i.e., to larger depths from the sample surface) represents its diffusion through the Cr layer to the underlying $B_{12}P_2$. The broadening of the Cr peak is consistent with such interdiffusion. Both B and P edges are shifted to higher energies, indicating that not only does $B_{12}P_2$ react with Cr/Pt, but both B and P atoms are mobile at 700 °C and rapidly diffuse toward the surface. P diffuses completely to the sample surface, as evidenced by a peak at 1.20 MeV, corresponding to scattering from P atoms at the sample surface. In addition to the morphology change, the large amount of mixing and fast diffusion of the species involved at this temperature is consistent with the formation of a liquid eutectic.

After annealing at 700 °C for 30 s, the specific contact resistance was 2×10^{-4} Ω cm^2. In an attempt to further lower the contact resistance, the contacts were annealed repeatedly at 700 °C in 30 s increments. Higher annealing temperatures were avoided to prevent dewetting and lateral spreading of the contact. After annealing for two cumulative minutes at 700 °C, the contact resistance did not decrease but rather slightly increased to 3×10^{-4} Ω cm^2 with no further change in surface morphology.

The minimum specific contact resistance for Cr/Pt to $B_{12}P_2$ in this study is similar to the minimum values of ~ 2–3×10^{-4} Ω cm^2 reported by Wang *et al.*[10] for Cr/Pt contacts to $B_{12}As_2$. In both studies, the lowest contact resistance is attained after annealing at 700 °C for 30 s. $B_{12}P_2$ and $B_{12}As_2$ could be expected to behave similarly due to their similar structure and comparable band gaps of 3.35 (Ref. 1) and 3.37 eV,[30] respectively. Also, since both materials are largely composed of B, the contact resistances may also be dominated by B-Cr and B-Pt interactions, thus masking differences between each material. In contrast, however, Cr/Pt contacts to $B_{12}As_2$ are suggested to be ohmic before annealing,[10] while Cr/Pt contacts to $B_{12}P_2$ only become ohmic after annealing at 700 °C.

B. Ni/Au contacts

The Ni/Au contacts were annealed sequentially at 200, 300, 400, 500, 600, 700, and 800 °C for 30 s at each temperature. As can be seen in Fig. 4, the contacts are ohmic before any annealing. The annealing progression of the *I-V* curve can be broken into two regimes. In the first regime, annealing up to 400 °C causes essentially no change in the *I-V* curve. A step change in the *I-V* characteristics occurs after annealing at 500 °C for 30 s, marking a second regime where the specific contact resistance decreases by an order of magnitude. Subsequently, higher temperature anneals, however, do not drastically affect the *I-V* curve. This effect is better illustrated in Fig. 5, showing the specific contact resistance

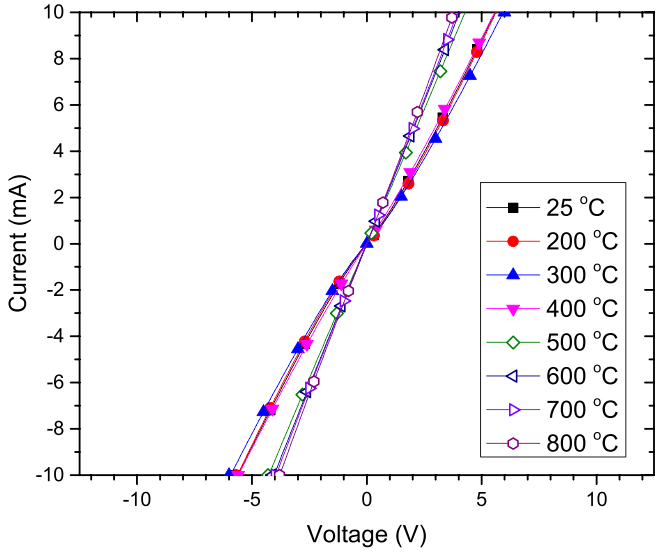

FIG. 4. (Color online) Progression of the current–voltage curve for different annealing temperatures for Ni/Au contacts with a spacing of 10 μm. After annealing at 500 °C for 30 s, the curves become steeper (open markers), a result of reducing the contact resistance.

as a function of anneal temperature, with specific contact resistance values of $\sim 2\text{–}4 \times 10^{-3}$ Ω cm^2 and $\sim 2\text{–}4 \times 10^{-4}$ Ω cm^2 in the low and high temperature regimes, respectively. The specific contact resistance is only slightly lowered by annealing above 500 °C. Such a step-like change in the annealing temperature range of 400–500 °C is most likely due to a metal-semiconductor interfacial reaction.

After annealing at 800 °C for 30 s, the metal contacts display visible signs of reaction with $B_{12}P_2$ around the edges of contact pads. Figure 6 shows the edge of a Ni/Au contact prior to annealing and the edge of two contacts originally spaced 5 μm apart after annealing at 800 °C for 30 s. The edge of the contacts clearly diffuses outward, and droplets form around the periphery, suggesting that the edge reaches

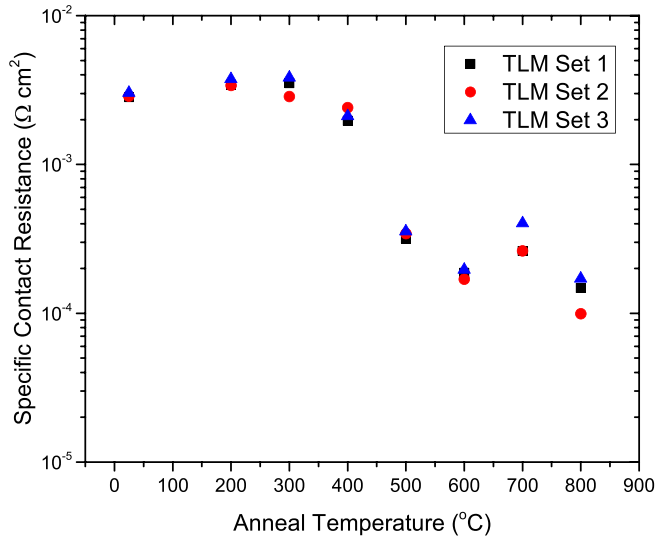

FIG. 5. (Color online) Change in the specific contact resistance of Ni/Au contacts as a function of anneal temperature. Three sets of TLM patterns were tested after each anneal.

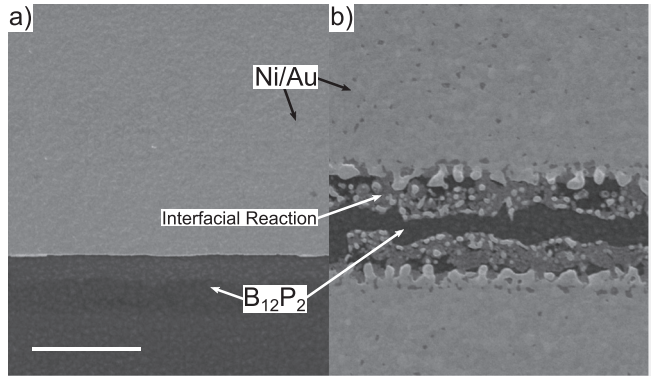

FIG. 6. SEM micrograph of (a) Ni/Au contact edges before annealing and (b) space between two Ni/Au contacts originally 5 μm wide after annealing at 800 °C for 30 s. The edges of the contacts become rough and spread outward after annealing. The scale bar is 6 μm.

a eutectic during the annealing. From the Ni-Au phase diagram,[31] the droplets at the edge cannot be a result of a eutectic caused solely by the metals since the Ni-Au eutectic is above 950 °C. Therefore, the metal must be reacting with the underlying $B_{12}P_2$. Since none of the binary phase diagrams of the elements of interest have eutectics below 850 °C,[32,33] the droplets must be a three or more component mixture. The center of the contact remains intact but has speckles over the surface [Fig. 6(b)]. This may be caused by Ni diffusion and segregation at the sample surface, which is common for Ni/Au contacts on other materials such as GaN.[34–37]

To further investigate the interfaces in the Au/Ni/$B_{12}P_2$ system, RBS was performed on a sample before any heat treatment and after the 500 °C anneal, which caused a major change in the *I-V* characteristics. The RBS spectra are shown in Fig. 7. Before annealing, the spectrum reflects nonintermixed layers of Au and Ni on $B_{12}P_2$. Again, the Ni, P, and B peak edges (roughly located at 1.45, 1.0, and 0.32 MeV, respectively) are shifted to lower energies since those elements are located beneath the sample surface. During

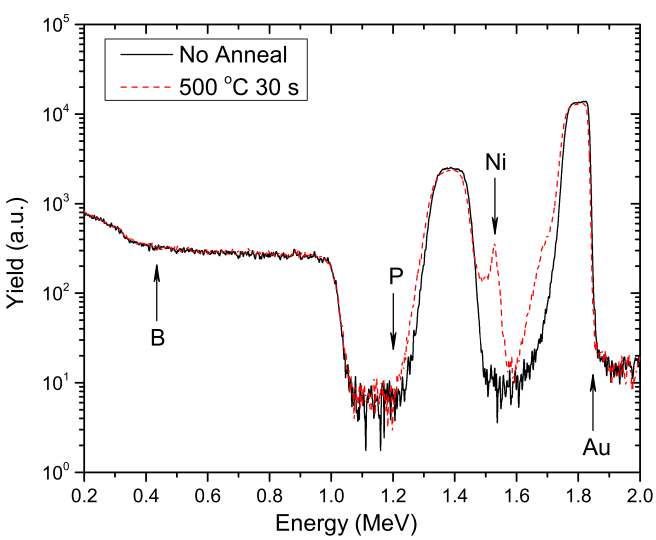

FIG. 7. (Color online) Semilog plot of RBS spectra for Ni/Au contacts before any heat treatment and after annealing at 500 °C for 30 s. The positions of the surface peaks of Au, Ni, P, and B are denoted by arrows.

annealing, Au and Ni layers interdiffuse, as indicated by the broadening of the Au peak to lower energies and the Ni peak to higher energies. In addition, after the anneal, a small, sharp Ni peak is present at the energy corresponding to the sample surface, confirming Ni diffusion to the surface of the contact. A slight broadening of the Ni peak to lower energies after the 500 °C anneal suggests lateral nonuniformity in the Ni layer thickness. This is consistent with SEM observations [Fig. 6(b)]. The fact that RBS signals from B and P are unchanged upon annealing at 500 °C indicates that the reaction layer thickness and diffusion length of these elements must be less than ~25 nm—the detection limit of this RBS measurement. In spectra taken after anneals up to 800 °C (not shown), the P peak is shifted to higher energies and confirms an increase of the reaction layer thickness.

The above results show that annealing at 500 °C for 30 s is sufficient to lower the Ni/Au contact resistance without spreading of the metal contacts along the $B_{12}P_2$ surface. This anneal temperature is also low enough to avoid the annealing-induced reduction in sheet resistivity reported by Wang *et al.*[10] while still attaining reasonably low contact resistances. Hence, annealing at 500 °C for 30 s is the optimum procedure in this study.

C. Comparison of Ni/Au and Cr/Pt contacts

Ni/Au and Cr/Pt contacts differ in several key ways. First, unlike Cr/Pt, the as-deposited Ni/Au contacts are ohmic. The measured sheet resistance between the Cr/Pt sample and Ni/Au sample are not significantly different, and variations in the $B_{12}P_2$ conductivity cannot be attributed for the difference in conduction. In fact, the sheet resistance for the Ni/Au film is slightly greater (3.2×10^3 Ω/□ versus 1.8×10^3 Ω/□ for Cr/Pt). One possible explanation for the difference in the conduction mechanism for the as-deposited condition is that Ni has a higher work function than Cr (as shown in Table I) and lowers the barrier height. A second explanation is that Cr is more susceptible to oxidation (for instance, from residual water vapor in the metal evaporation system) and could form an oxide barrier between $B_{12}P_2$ and Cr. Another difference between the Ni/Au and Cr/Pt contacts is the alloying characteristics necessary for low resistance contacts. The Cr/Pt contacts not only need to react with the surface of $B_{12}P_2$ to become ohmic, but the contacts must react to a much greater degree than Ni/Au to achieve a specific contact resistance on the order of 10^{-4} Ω cm^2. Further, Cr/Pt contacts redistribute both B and P throughout the depth of the contact. At 500 °C, B and P are essentially immobile in the Ni/Au system.

IV. CONCLUSION

Cr/Pt and Ni/Au ohmic contacts to *p*-type $B_{12}P_2$ were developed. Cr/Pt contacts became ohmic after annealing at 700 °C for 30 s with a specific contact resistance of 2×10^{-4} Ω cm^2. RBS demonstrates that Cr, Pt, B, and P intermix before ohmic conduction is achieved. Ni/Au contacts, however, are ohmic in the as-deposited condition and have a specific contact resistance of 3×10^{-4} Ω cm^2 after annealing at 500 °C for 30 s. RBS indicates that the reaction layer between Ni and $B_{12}P_2$ is less than ~25 nm thick and that Ni diffuses to the sample surface. Ni/Au contacts display superior properties than Cr/Pt contacts, including ohmic conduction prior to annealing, better thermal stability, and a similar contact resistance at a lower anneal temperature that is also below the observed temperature that causes a reduction in sheet resistance in icosahedral borides.

In future work, increasing the dopant level in $B_{12}P_2$ may aid in reducing the specific contact resistance. Si, a *p*-type dopant in $B_{12}As_2$, could be coevaporated with Ni. Alternatively a thin Si film could be evaporated prior to Ni evaporation. While sintering the contact, Si may diffuse into the $B_{12}P_2$ directly beneath the contact, locally increase the doping concentration, and lower the contact resistance. Such a scheme may become even more important when creating ohmic contacts to $B_{12}P_2$ that has a lower background doping level.

ACKNOWLEDGMENTS

This work was performed under the auspices of the U.S. Department of Energy by Lawrence Livermore National Laboratory under Contract Nos. DE-AC52-07NA27344 and LLNL-JRNL-666166. Material growth was supported by the U.S. Department of Energy, Office of Basic Energy Sciences under Award No. DE-SC0005156.

[1]G. A. Slack, T. F. McNelly, and E. A. Taft, J. Phys. Chem. Solids **44**, 1009 (1983).
[2]D. Emin, J. Solid State Chem. **179**, 2791 (2006).
[3]M. Carrard, D. Emin, and L. Zuppiroli, Phys. Rev. B **51**, 11270 (1995).
[4]Y. Zhang *et al.*, *MRS Proceedings* (Cambridge University, Cambridge, United Kingdom, 2011), Vol. 1307, p. mrsf10-1307.
[5]Y. Zhang *et al.*, J. Cryst. Growth **352**, 3 (2012).
[6]Z. Xu, J. H. Edgar, D. C. Look, S. Baumann, R. Bleiler, S. H. Wang, and S. E. Mohney, J. Appl. Phys. **101**, 053710 (2007).
[7]Y. Gong, M. Tapajna, S. Bakalova, Y. Zhang, J. H. Edgar, M. Dudley, M. Hopkins, and M. Kuball, Appl. Phys. Lett. **96**, 223506 (2010).
[8]J. O. Song, J.-S. Ha, and T.-Y. Seong, IEEE Trans. Electron Devices **57**, 42 (2010).
[9]Y. Ino, S. Nishimura, M. Hirai, S. Matsumoto, and K. Terashima, Jpn. J. Appl. Phys. **52**, 031201 (2013).
[10]S. H. Wang, E. M. Lysczek, B. Liu, S. E. Mohney, Z. Xu, R. Nagarajan, and J. H. Edgar, Appl. Phys. Lett. **87**, 042103 (2005).
[11]Y. Kumashiro, T. Yokoyama, T. Sakamoto, and T. Fujita, J. Solid State Chem. **133**, 269 (1997).
[12]Y. Kumashiro, H. Yoshizawa, and K. Shirai, JJAP Ser. **10**, 166 (1994).
[13]M. Takigawa, M. Hirayama, and K. Shohno, Jpn. J. Appl. Phys. **12**, 1504 (1973).
[14]S. N. L'vov, V. F. Nemchenko, P. S. Kislyi, T. S. Verkhoglyadova, and T. Y. Kosolapova, Sov. Powder Metall. Met. Ceram. **1**, 243 (1962).
[15]*Dictionary of Inorganic Compounds*, 1st ed., edited by J. E. Macintyre (Chapman and Hall/CRC, London, UK, 1992), Vol. 5, p. 3082.
[16]H. Okamoto, J. Phase Equilib. **24**, 480 (2003).
[17]M. Venkatraman and J. P. Neumann, Bull. Alloy Phase Diag. **11**, 430 (1990).
[18]B. Predel, in *B-Ba C-Zr, Landolt-Brnstein—Group IV Physical Chemistry*, edited by O. Madelung (Springer, Berlin, Heidelberg, 1992), Vol. 5b, pp. 1–3.
[19]H. Okamoto, Bull. Alloy Phase Diag. **11**, 511 (1990).
[20]M. D. Smolin, V. G. Grebenkina, Y. M. Goryachev, L. I. Panov, and E. I. Shvartsman, Sov. Powder Metall. Met. Ceram. **21**, 662 (1982).
[21]I. Shirotani, E. Takahashi, N. Mukai, K. Nozawa, M. Kinoshita, T. Yagi, K. Suzuki, T. Enoki, and S. Hino, Jpn. J. Appl. Phys. **32**, 294 (1993).
[22]N. Kobayashi, Y. Kumashiro, P. Revesz, J. Li, and J. W. Mayer, Appl. Phys. Lett. **54**, 1914 (1989).

[23]R. I. Stearns and P. E. Greene, J. Electrochem. Soc. **112**, 1239 (1965).
[24]U. Nwagwu, "Flux growth and characteristics of cubic boron phosphide," Master's thesis (Kansas State University, 2012).
[25]T. L. Chu, M. Gill, and R. K. Smeltzer, J. Cryst. Growth **33**, 53 (1976).
[26]D. K. Schroder, *Semiconductor Material and Device Characterization*, 2nd ed. (Wiley-Interscience, New York, 1993), Chap. 3, pp. 133–199.
[27]F. A. Padovani and R. Stratton, Solid-State Electron. **9**, 695 (1966).
[28]D. Eastman, Phys. Rev. B **2**, 1 (1970).
[29]M. Venkatraman and J. P. Neumann, Bill. Alloy Phase Diag. **11**, 16 (1990).
[30]P. B. Klein, U. Nwagwu, J. H. Edgar, and J. A. Freitas, Jr., J. Appl. Phys. **112**, 013508 (2012).
[31]T. A. Hall and A. A. Johnson, J. Less Common Met. **141**, L19 (1988).
[32]H. Okamoto, J. Phase Equilib. **21**, 210 (2000).
[33]O. Teppa and P. Taskinen, Mater. Sci. Technol. **9**, 205 (1993).
[34]H. W. Jang, S. Y. Kim, and J.-L. Lee, J. Appl. Phys. **94**, 1748 (2003).
[35]A. Motayed, A. V. Davydov, L. A. Bendersky, M. C. Wood, M. A. Derenge, D. F. Wang, K. A. Jones, and S. N. Mohammad, J. Appl. Phys. **92**, 5218 (2002).
[36]Y. Koide, T. Maeda, T. Kawakami, S. Fujita, T. Uemura, N. Shibata, and M. Murakami, J. Electron. Mater. **28**, 341 (1999).
[37]J.-K. Ho, C.-S. Jong, C. C. Chiu, C.-N. Huang, K.-K. Shih, L.-C. Chen, F.-R. Chen, and J.-J. Kai, J. Appl. Phys. **86**, 4491 (1999).